Impact of Organoclay and Maleated Polyethylene on the Rheology and Instabilities in the Extrusion of High Density Polyethylene

Ayuba A. Adesina, Ibnelwaleed A. Hussein

Department of Chemical Engineering, King Fahd University of Petroleum and Minerals, 31261 Dhahran, Saudi Arabia

Received 20 February 2011; accepted 18 March 2011
DOI 10.1002/app.34523
Published online 8 August 2011 in Wiley Online Library (wileyonlinelibrary.com).

ABSTRACT: The impact of organoclay on the rheology and extrusion of high density polyethylene (HDPE) was studied. Organoclay effect was studied at very low clay loading (≤0.1 wt %) while serving as a processing aid. A special design slit die with three transducers was used in the study of the extrusion melt instabilities. The rheological results showed that normal stress difference of HDPE was reduced during steady shear rate and stress growth tests when organoclay (≤0.1 wt %) was added. The extensional strain and stress growth of HDPE reduced with the addition of organoclay. So, organoclay (≤0.1 wt %) has an effect on the shear and extensional rheology of HDPE. The intensity of the melt instability was characterized with both a moment analysis and distortion factor (DF) from an advanced Fourier transform analysis. Both showed the same trends in the characterization of the pressure fluctuations in the die. Generally, addition of organoclay (≤0.1 wt %) to HDPE led to the reduction in DF. The ratio of first and second moment analyses became reduced as well. The results quantified the extent of elimination of gross melt fracture in HDPE by organoclay. Also, the extrusion pressure was reduced with organoclay (≤0.1 wt %) inclusion hence more throughput. There was a good correlation between rheology and extrusion. Both showed that the platy-like organoclay streamlined the melt flow. However, the maleated polyethylene added as a compatibilizer did not give substantial synergistic effect.
 J Appl Polym Sci 123: 866–878, 2012

Key words: organoclay; melt instability; extrusion; polyethylene; distortion factor; processing aid

INTRODUCTION

In polymer processing, the continuous increase in the production rate at low power consumption during the extrusion process is limited by the onset of polymer melt fractures. The onset of surface and/or gross melt instabilities at relatively high shear rates made the glossy polymer surface rough. Many studies had been carried out in the past to understand the causes, effects and ways to eliminate or postpone these instabilities.[1–3] Methods used to solve these instabilities, among others, include modification of the extruder especially the die head,[4–7] conditioning the die surface,[8–12] modification of the polymer[13–16] and addition of processing additives.[17] The processing additives often added, depending on the types of instabilities, include fluoropolymers,[18–20] stearates,[17] silicon-based additives and boron nitride.[21–24] Other materials such as carbon nanotube[25,26] also have indirect improvement on the polymer melt instabilities. Recently, it was proposed that organoclays[27] can also be a very good processing additive for polyolefins. Researchers, at times, combine several additives to tackle different stages of melt fractures.[27,28]

Gross melt fracture is a bulk instability which occurs in polymers at high shear rates. This type of melt fracture becomes important and underscores the other types of instabilities in processes like extrusion with post pelletization. Parts of the major efforts being adopted to eliminate or postpone gross melt fracture include the addition of platy-like boron nitride and very recently, organoclay. It was also reported that dicumyl peroxide[29,30] and carbon nanotube[25] can also postpone the occurrence of melt fracture in polyethylene to higher shear rate. Boron nitride can eliminate both sharkskin and gross melt fracture depending on the ratio of the dispersive and nondispersive components of the surface energy of the boron nitride.[23,31–33] Generally, the addition of

Correspondence to: I. A. Hussein (ihussein@kfupm.edu.sa).
Contract grant sponsor: King Abdul Aziz City for Science and Technology (KACST); contract grant number: AT-27-107.
Contract grant sponsor: King Fahd University of Petroleum and Minerals (KFUPM).

boron nitride to the host polymer did not result in the decrease of the extrusion pressure but enhanced the temperature effect[33] during the extrusion to eliminate the melt fracture. It was observed that as the concentration of boron nitride in fluoropolymer processing decreased, the critical shear rates at which melt fracture set-in decreased.[21,22] The reverse was the case when boron nitride was used as a processing additive in polyolefin processing.[22] Recently, the single-walled and double-walled carbon nanotubes effects on the processing of polyolefins were studied. They modified the sharkskin and spurt instabilities of the parent polyolefins at low shear rates and completely eliminated the gross melt fracture at high shear rates.[25] It was observed that there was a complex interaction between the types of branching and the carbon nanotubes. Similar to what was observed in the use of the boron nitride, the critical stress threshold was not affected by the addition of carbon nanotubes.[25] Low carbon nanotube loading less than 0.1 wt % can eliminate low shear rate instability-sharkskin. However, a carbon nanotube loading more that 3 wt % must be used to see its effectiveness in eliminating or postponing high shear rate instability - gross melt fracture. Palza et al. further observed that the addition of a carbon nanotube reduced the die swell of the parent polymer due to its impact on first normal stresses and such effect may influence the morphology changes in the polymer melt instabilities.[25] The carbon nanotube loading was relatively high so it may not be a good processing aid when compared to the quantity of other processing nano-additives, which are often far less than 0.5 wt %.[27]

There appears to be little published literatures on the subject of organoclay as a processing aid in polymers.[27,34] In their works, capillary rheometer was used during the processing. It was observed that organoclay eliminated surface melt fracture-sharkskin and postponed the critical shear rate at which the gross melt fracture occurred. The organoclay was able to postpone the bulk fracture because it reduced the extensional stresses which often caused such instability in polyolefins.[27] These effects were observed in the capillary and crosshead dies attached to the capillary rheometer. Impact of organoclay on the extrusion pressure was characterized by a complex relationship between the parent polymers and types of dies. After careful observation of the Hatzikiriakos et al. work, we noticed that the addition of 0.1 wt % organoclay to HDPE had no effect on the extrusion pressure regardless of the types of dies.[27]

In this study, the effect of organoclay on the continuous extrusion of HDPE in a single screw extruder with a specially designed slit die as a head is studied. The slit die has three highly sensitive piezoelectric pressure transducers along its length. This type of system has not been used before to study the impact of organoclay on melt instabilities. Another key point in the effective elimination or postponement of melt instabilities is the dispersion of organoclay in the polyolefin matrix. Two different mixing techniques are examined in this work. The effect of compositions ($\leq$0.1 wt %) of organoclay in the polymer matrix on shear and extensional rheology is further investigated and correlated to instabilities in the extrusion process. It should be noted it would be redundant to study higher compositions because organoclay is being proposed as a new processing aid for polyolefin extrusion.

EXPERIMENTAL

Materials

Commercial grade HDPE (relative density = 0.952, melting point = 132°C and melt flow index = 0.05 g/10 min at 190°C and 2.16 kg load) used in this work was supplied by Saudi Basic Industries Corp. (SABIC). It has an average-weight molecular weight (M_w) of 285 kg/mol with molecular weight distribution of 26.5. Organoclay used in this work was Cloisite® 15A (C15A) obtained from Southern Clay. The surfactant modifier in C15A was dimethyl, dehydrogenated tallow, quaternary ammonium salt. The concentration of the modifier was 125 meq/100 g clay (i.e., the concentration modifier is 0.125 g per 100 g clay). According to the supplier, the d_{001} spacing of C15A was 31.5 Angstrom. C15A was chosen for this work because it is one of the most easily dispersed organoclay in polyolefin.[35] Polyethylene grafted maleic anhydride (PE-*g*-MA) from Aldrich was used as a compatibilizer. This was used in the received form without any modification. The maleic anhydride as a comonomer in PE-*g*-MA was $\sim$ 3 wt %. The compatibilizer viscosity was 4.5 Pa s at 140°C with relative density of 0.925. Its melting point and saponification value were 105°C and 33 mg KOH/g, respectively. Various researchers had previously used PE-*g*-MA to facilitate the dispersion of organoclay in polyethylene[36–40] The antioxidant used in this work was a 50/50 weight blend of Irganox 1010 and Irgafos 168 from Ciba-Geigy Speciality.

Melt blending and morphology characterization

The Brabender 50 EHT mixer supplied with a Plastograph was used in the preparation of the nanocomposites. The organoclays were first heated in a vacuum oven at 108°C for more than 24 h to remove physico adsorbed water. HDPE was grinded and physically premixed with organoclay and antioxidant. Then, a master batch with and without

compatibilizer was prepared in the Brabender mixer. A desired final concentration of a particular blend was obtained by mixing additional virgin HDPE to the master batch using the same mixer. The blending was done at a temperature of 200°C and screw speed of 50 rpm for 10 min. About 0.1 wt % of antioxidant was added to avoid degradation of the nanocomposite during the melt blending.

The amount of PE-*g*-MA in the blends was fixed such that its ratio to C15A content was 3 : 1. The compositions of the prepared HDPE-C15A nanocomposites (HDPE-x) were as listed in Table I. HDPE-1000 represented a nanocomposite based on HPDE with 0.1 wt % C15A without a compatibilizer. HDPE-1000w represented a nanocomposite based on HPDE containing 0.1 wt % C15A and 0.3 wt % PE-*g*-MA.

The structures of the HDPE-C15A nanocomposites were characterized by FE-SEM and XRD. The XRD analysis was performed on XRD-6000 Shimadzu diffractometer with CuKα radiation ($\lambda = 0.154$ nm) in a reflection mode, operating at 40 kV and 30 mA. Scanning speed of 1°/min was used. The scan range was 2–10° at room temperature.

Scanning electron micrographs were obtained with FE-SEM Nova^{TM} Nanosem 230. It is possible to achieve ultra-high resolution on nonconductive nano-materials with Nova^{TM} Nanosem 230. The SEM samples were made into thin films and etched for 4 h. The etching solution was made from a solution of $H_2SO_4/H_3PO_4/H_2O$ (10/4/1) and 0.01 g/mL $KMnO_4$ as described by Szadi et al.[36] The etched samples were then covered with gold to make them conductive.

Rheological measurement

The samples for the shear experiments were prepared from melt blended samples at a temperature of 200°C and a pressure of up to 30 Pa was applied in a Carver press. The disc samples with dimensions of 25 mm diameter and 2 mm thickness were prepared for shear rheology. An ARES rheometer was used for all the rheological measurements, namely a controlled strain rheometer equipped with heavy transducer (range 0.02–20 *N* for normal force; 2×10^{-5} to 2×10^{-1} Nm for torque). The linear and nonlinear viscoelastic experiments were performed using 25 mm parallel plates. The plates were heated for at least 20 min to equilibrate the temperature. For reproducibility of results, a presteady shear rate of 0.1/s was applied for 20 s for all the tests in the parallel plates and time delay of 100 s before the actual tests. Different rheological tests were conducted to study the material properties under different rheological conditions.

Strain sweep tests were conducted for all the samples to determine the linear viscoelastic region.

TABLE 1
HDPE Containing Different Compositions of C15A and Compatibilizer

	HDPE (wt %)	PE-g-MA (wt %)	CI5A (parts per million)
Pure-HDPE	100	0	0
HDPE+Compatibilizer	99.7	0.3	0
HDPE-500	100	0	500
HDPE-1000	100	0	1000
HDPE-1000w	99.7	0.3	1000

A Strain range of 10–400% with shear amplitude of 1 rad/s was used. Frequency sweep experiments were performed in the frequency range between 0.01 rad/s and 100 rad/s. The applied strain was 20%. The strain was within the linear regime as determined by the strain sweep test. Auto tension was applied during the test to keep the upper plate in contact with the sample throughout the experiment. Steady shear rate sweep tests were conducted between 0.001 and 1 s^{-1}. The maximum shear rate was limited by the secondary flow-induced instabilities generated at the melt sample periphery edges.[37] The delay and measurement time for each strain rate was 30 s. A Rosand RH7 twin bore capillary rheometer was used at high shear rates to get more rheological viscosity data. The diameter (D) and entrance angle of the long and short capillary dies were 2 mm and 180°, respectively. The lengths of the long (L_l) and short dies (L_s) were 16 and 4 mm, respectively. If P_L is the pressure drop across the long die and P_s is the pressure drop across the short die, the orifice pressure drop (P_o) was calculated by interpolation using:

$$P_o = P_s - \frac{P_L - P_s}{L_l - L_s} L_s \tag{1}$$

The true wall shear stress (σ_w) was determined via:

$$\sigma_w = \frac{(P_l - P_o)D}{4L_l} \tag{2}$$

The apparent wall shear rate ($\dot{\gamma}_a$) and true wall shear rate ($\dot{\gamma}_w$) were:

$$\dot{\gamma}_a = \frac{32Q}{\pi D^3} \quad \text{and} \quad \dot{\gamma}_w = \frac{1+3n}{4n} \tag{3}$$

where Q is the volume flow rate and n is the power law index.

The responses of the samples during stress growth were conducted to study the effect of organoclay on the nonlinear shear material function of HDPE. The imposed shear rate was 0.8 s^{-1}. Low shear rate was

used due to the limitation of the parallel plate geometry as mentioned earlier. An Extensional Viscosity Fixture (EVF) from ARES was used for the study of extensional rheology. The sample was prestretched with a strain rate of 0.4 s^{-1} to remove sagging. The sample was left in the fixture for 3 min to relax any accumulated stress before the start of the experiment. A Hencky strain rate of 10 s^{-1} and a temperature of 145°C were used for these experiments. Such a high Hencky strain rate and low temperature were necessary to observe the effect of organoclay on the extensional rheology of HDPE.

Set-up for melt flow instabilities

Extrusion was carried out in a single screw extruder 19/25D from a Brabender equipped with a specially developed slit die. The slit die has a dimension of 0.8 mm height, 20 mm width, and 160 mm length. The slit die has highly sensitive piezoelectric transducers located at three different positions. The positions of the transducers along the slit die were 30, 80, and 140 mm from the entrance of the die. The pressure and time resolutions of these transducers are of the order of 10^{-1} mbar and 1 ms, respectively. Details about the die were reported elsewhere.[7,14,38] However, this set-up was different from those reported earlier in two ways: First, the slit die in this work was attached to a single screw extruder; second, the die has larger dimensions as shown in Figure 1. It was developed with the help of Prof. Manfred Wilhelm of Karlsruhe Institute of Technology, Germany.

The measurements with the three highly sensitive piezoelectric transducers were done to specifically identify and analyze the time dependent pressure fluctuations associated with smooth polymer flow and melt flow instabilities. The time dependent pressure oscillations were collected by the use of these fast acquisition piezoelectric transducers combined with an oversampling technique to increase the noise to signal ratio. So, the 30,000 data points/channel was reduced to 100 data points/s using an oversampling rate of 300 data points/s. The oversampled time dependent pressure was further analyzed using a Fourier transformation. This resulted in a spectrum with a maximum intensity at a frequency of 0 Hz. This intensity corresponds directly to the mean value of the pressure. The pressure oscillation during melt flow instabilities can be observed as additional peaks, located at higher frequencies. Details of these advanced mathematical analyzes can be seen elsewhere.[14] In this work, both moment analyses and a distortion factor from a Fourier transform analysis were used in our analyses.

The moment analysis is often used to characterize the time dependent data. Generally, *k*-moment

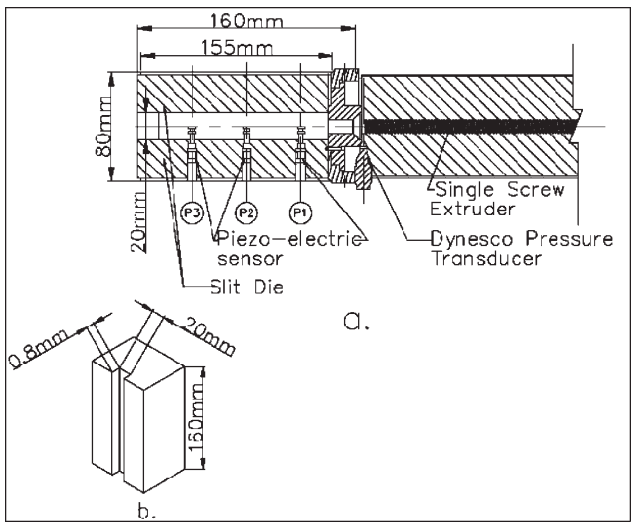

Figure 1 (a) Longitudinal section of the single screw extruder with slit die head having three highly sensitive piezoelectric pressure transducers along the die. This is the set-up for the study of melt instabilities during polymer extrusion. (b) The slit die with its dimensions.

$$m_k = \frac{1}{t_f - t_o} \int_{t_o}^{t_f} (p(t) - \bar{p})^k dt \tag{4}$$

where m_k is the *k*th moment of the pressure, $\bar{p}$ is the mean value which is the first moment around zero and $p(t)$ is the time dependent pressure signal. The second moment is the variance and its square root is the standard deviation. In this work, the ratio of the standard deviation divided by the mean of the pressure fluctuation will be used in the characterization of the melt instability.

A Fourier transform analysis (FT) is another alternative and growing advanced mathematical tool in the analysis of the inherent periodic contributions from the time dependent variables like pressure fluctuation along the die. The time dependent pressure can be analyzed as being a combination of different harmonic contributions as shown below:

$$p(t) = \bar{p} + \sum_{i \geq 1} l_i \cos(w_i t + \emptyset_i) \tag{5}$$

where $\bar{p}$ is the pressure mean value at $\frac{w}{2\pi} = 0$; $\frac{w_i}{2\pi}$, $\emptyset_i$, and l_i are the characteristic frequencies, phases, and amplitudes of the pressure fluctuation as quantified from the Fourier analysis of the processed signals, respectively. It is assumed that all the information related to the melt instability is included in these parameters. Details of the FT analysis can be seen in the work of Palza et al.[7,25] One of the most important parameters from the FT analysis in quantifying melt instabilities is the distortion factor (DF). This is

a measure of the relative pressure fluctuation (RPF) as defined in Eq. (6).

$$DF = \frac{\sum_{i\geq 1} l_i}{l_0} \tag{6}$$

l_0 represents the peak value at $w = 0$ and it is related to the pressure mean value. It should be noted that the summation of harmonics (amplitudes of the pressure fluctuations) is retained because there are higher harmonics with a magnitude of the same order as l_1.

There are three heating zones along the single screw extruder with a separate heating element for the slit die. The extrusion was done at temperature program 160-160-160-145°C where the screw and slit die were maintained at 160 and 145°C, respectively. The screw speed was varied up to the limit of the extruder. The piezoelectric transducer can only be used to obtain pressure fluctuation and not absolute pressure. Hence, the pressure drop (ΔP) across the slit die was measured with the Dynisco pressure transducer placed at the entrance of the slit die (Fig. 1). The maximum allowable pressure in the transducer was 70 MPa. The pressure data was collected via the acquisition program provided by the Brabender. The acquisition rate was 1 data per 20 s. The volumetric flow rate ($\dot{Q}$) was determined by collecting and measuring the ejected mass as a function of time. From the data, the wall shear stress (τ_{app}) and the apparent shear rate ($\dot{\gamma}_{app}$) were calculated using:

$$\tau_{app} = \Delta P \frac{h}{2l} \tag{7}$$

$$\dot{\gamma}_{app} = 6\frac{\dot{Q}}{bh^2} \tag{8}$$

where h, l, and b are the height, length, and width of the slit die, respectively.

RESULTS AND DISCUSSION

In this section, the outcomes of the morphological characterization, rheological tests and extrusion experiments on HDPE-C15A with and without a compatibilizer were discussed. The relationships between rheology and extrusion were combined to propose a mechanism through which the organoclay possibly influenced the HDPE extrusion in the wake of melt instabilities.

Morphological characterization

Figure 2 showed the wide-angle X-ray diffraction (WAXD) chromatogram for different composition of C15A in HDPE. It was observed that the C15A peaks

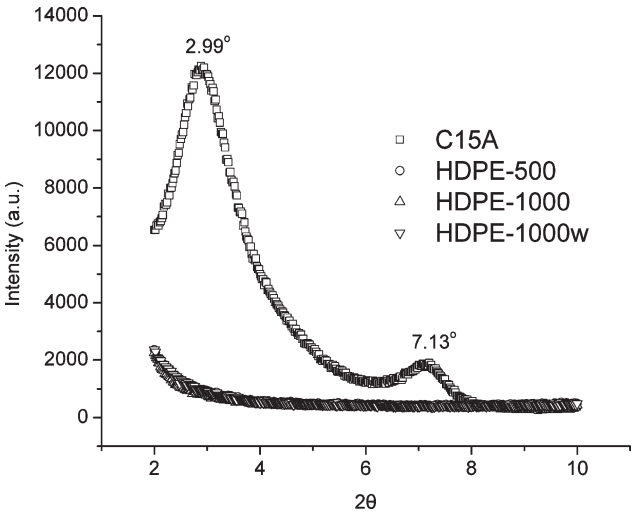

Figure 2 WAXD for HDPE, organoclay (C15A) and HDPE containing different clay loadings + compatibilizer.

at 2.99° ($d_{001} = 2.953$ nm) and 7.13° ($d_{002} = 1.239$ nm) disappeared. While one might infer that there was exfoliation of organoclay in all the nanocomposites, the dilution procedure might have also caused the disappearance. The addition of a compatibilizer did not lead to any difference in the chromatogram. The implications of these will be discussed during rheological testing and extrusion of the nanocomposites.

The SEM images of HDPE containing 0.1 wt % of organoclay with/without a compatibilizer were as shown in Figure 3(a,b). These results were obtained after etching. The figures showed that C15A was present and dispersed in both samples (HDPE-1000 and HDPE-1000w, respectively). Transmission electron microscopy was not carried out on the sample because it is too time consuming and costly for routine characterization. Moreover, we are not interested in the type of dispersion since the instability study would be carried out in an extruder at high shear rates. Such extrusion will further lead to the dispersion of the organoclay. These images supported the XRD results. However, the surface impact of the etching solution was very obvious in the chromatograms.

Rheological characterization

In the rheological characterization, both shear and extensional rheology were conducted. The tests were designed to comprehensively examine whether organoclay truly impacts the rheology of HDPE. The influence of the compatibilizer on the linear and nonlinear material properties of HDPE were discussed as well.

Shear rheology

The addition of organoclay and a compatibilizer to HDPE reduced the stress responsible for HDPE

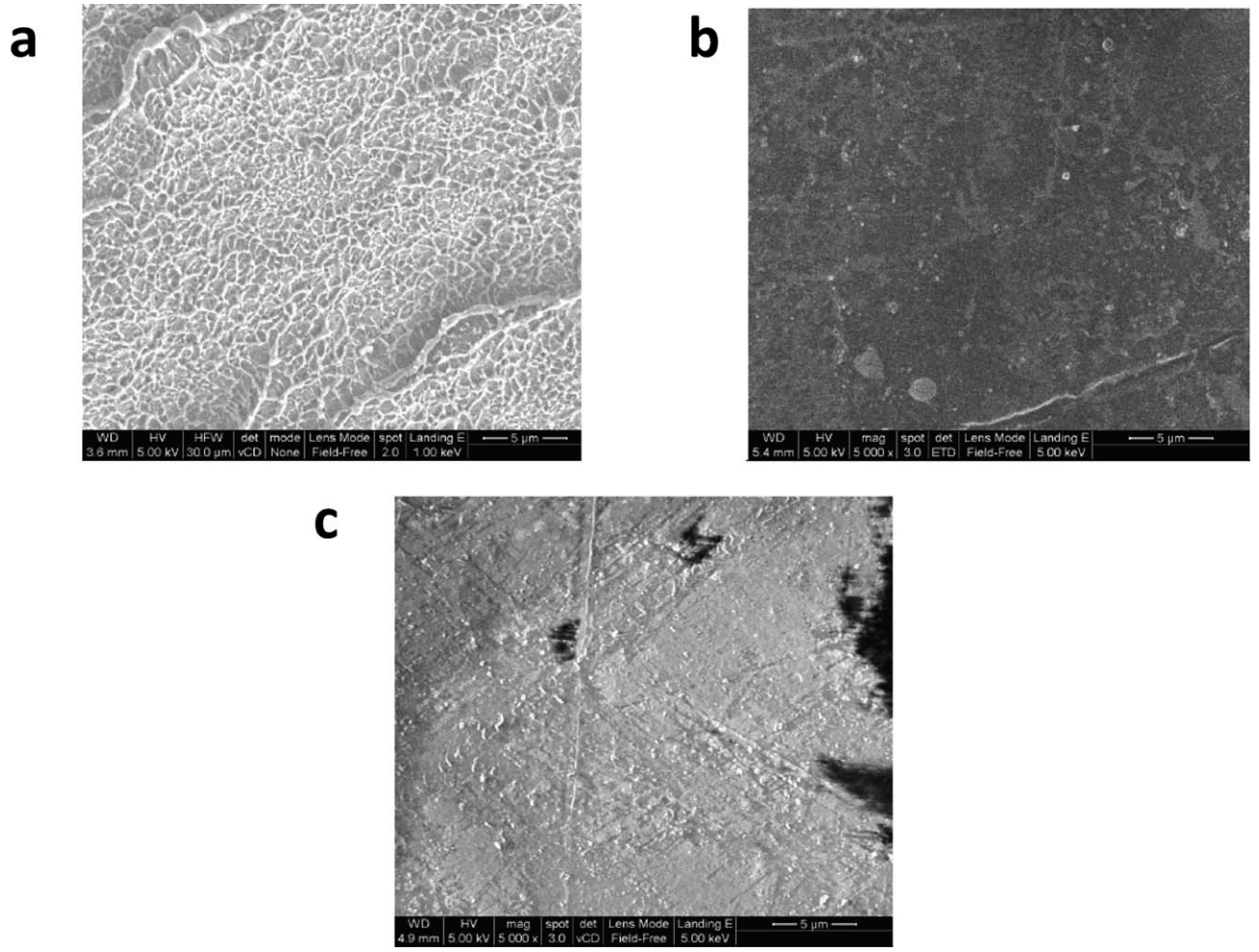

Figure 3 Scanning Electron Micrograph for (a) HDPE with 0.1 wt % C15A and (b) HDPE with 0.1 wt % C15A + 0.3 wt % compatibilizer.

deformation during strain sweep tests. The inclusion of 0.1 wt % of C15A to HDPE (HDPE-1000) caused a very small decrease of 5% in the relaxation modulus of HDPE (figure not shown). Such a decrease might be neglected because it was discovered that tan(δ) for the plots were well reproducible with ±2% difference. However, as the clay loading decreased, the relaxation modulus also decreased both at linear and nonlinear regimes. The reduction caused by the addition of 0.05 wt % C15A was as shown in Figure 4. The reduction was ~ 21% throughout the strain range considered in this work. The inclusion of a 0.3 wt % compatibilizer alone to HDPE also decreased the relaxation modulus of HDPE up to 20% (figure not shown).

A representative frequency sweep plot for virgin HDPE and addition of low amount of C15A was as shown in Figure 5. The crossover frequencies for all the samples were of the same order. At high frequencies above the crossover frequency, the elastic and viscous moduli were the same for all samples. Below the crossover frequency, the effect of organoclay began to appear as in Figure 5 for HDPE-500. With the addition of 0.1 wt % C15A to HDPE (HDPE-1000), the decrease in the moduli was not

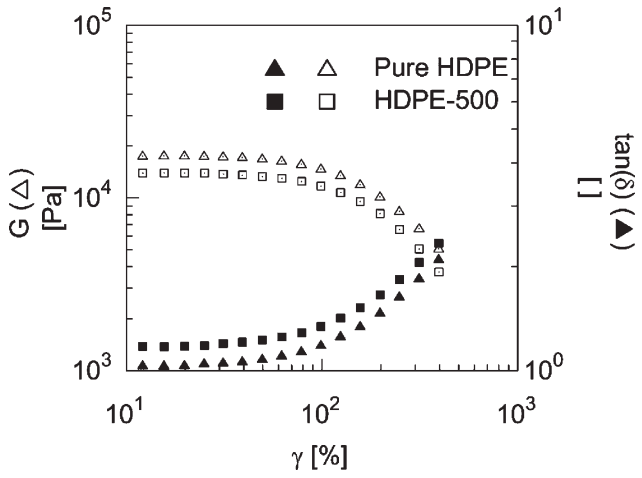

Figure 4 Relaxation modulus versus strain during strain sweep test for Pure HDPE and HDPE with 0.05 wt % organoclay.

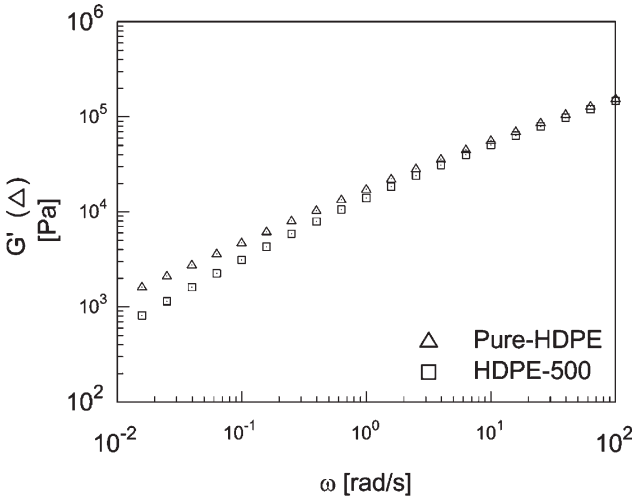

Figure 5 Dynamic frequency sweep of pure HDPE and HDPE with 0.05 wt % organoclay.

pronounced (figure not shown). The decrease was within the range of data reproducibility, namely 6%. This was in agreement with the result reported in the work of Hatzikiriakos et al. when they used 0.1 wt % of organoclay.[27] They concluded based on the result that a small addition of organoclay into polyolefins has no effect on the shear rheological properties of the polymers.[27] However, Figure 5 showed that as the clay loading was decreased to 0.05 wt % the elastic modulus decreased. At a frequency of 5 rad/s, the elastic modulus of HDPE decreased by 15% while it was 50% at a frequency of 0.015 rad/s. This was an indication that the linear viscoelastic properties of the polymers were affected by the addition of small amounts of C15A less that 0.1 wt %. An Addition of 0.3 wt % compatibilizer to HDPE also lowered the moduli at low frequencies. Hence, there was a further slight decrease in the elastic modulus of HDPE-1000 with the addition of a compatibilizer (figure not shown). Terminal plateau was not detected in Figure 5 because the use of HDPE was highly linear. Percolation threshold was absent in all the rheological plots because the amount of clay (less than 0.1 wt %) added to HDPE was very small to lead to a percolation network.

The severe impediment to the lateral motion of HDPE molecules during steady shear rate test led to the high zero-shear rate viscosity shown in Figure 6. A Cross model as defined in Eq. (9) was used in the fitness of shear rate dependent viscosity.

$$\eta = \frac{\eta_o}{1 + (C\dot{\gamma})^m} \tag{9}$$

η_o is the zero shear viscosity in Pa s, m is the (Cross) rate constant (dimensionless) and C is the cross time constant (or consistency) in second. C^{-1} is the inverse of cross time constant. It is the critical shear rate that shows the onset shear rate for shear thinning.

Table II gave the summary of the Cross model parameters for all the samples. From the table, the zero-shear viscosity reduced with the addition of organoclay and a compatibilizer. For instance, at clay loading of 0.1 wt %, the zero-shear viscosity of HDPE reduced by 16%. There was a further decrease of up to 44% when the clay loading was reduced to 0.05 wt %. The observed trends became important when it was noticed that the experimental data was reproducible within error margin less than 6%. At the shear thinning region, the cross rate constant and critical shear rate for the onset of the shear thinning were of the same order for all the samples. The capillary rheometer results (open legends in Fig. 6) showed that at higher shear rate, there was a slight decrease in the shear viscosity due to the addition organoclay especially with 0.05 wt % clay loading. Another observable trend at the shear-thinning region was the effect of organoclay on normal stress differences in Figure 7. The data reproducibility for the experiment was within 10%. Despite the high experimental error, the organoclay reduced the normal stress differences in HDPE. For instance, the normal stress difference in HDPE was reduced by 27% (at shear rate = 0.04/s) when 0.1 wt % organoclay was added. There was a further decrease of up to 33% when the clay loading was decreased to 0.05 wt %. The reason for the reduction in the normal stress difference might likely be as a result of the decrease in the elastic component of the polymer as previously discussed. The compatibilizer had an effect on the

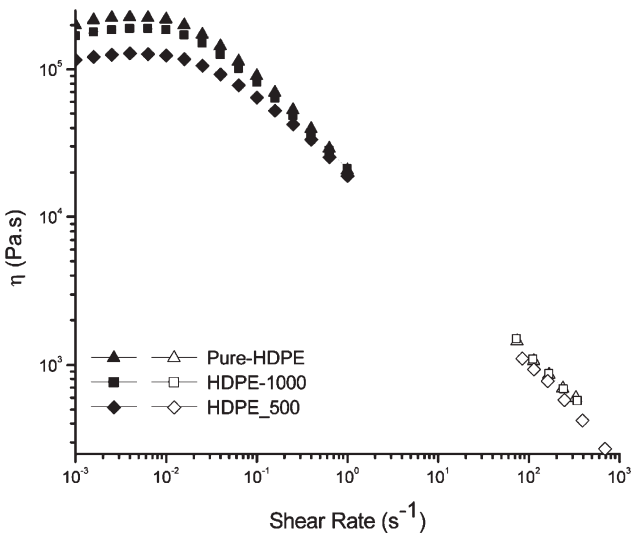

Figure 6 Effect of different clay loadings on the viscosity (η) of HDPE during steady shear rate sweep test in parallel plates (filled legend) and capillary rheometry (open legend).

TABLE 2
Cross Model Parameters for Pure-HDPE and its C15A Nanocomposites

Cross model parameters	Pure-HDPE	HDPE-compatibilizer	HDPE-1000	HDPE-1000w	HDPE-500
η_0 (Pa.s)	236180.0	146740.0	197010.0	133610.0	132290.0
M	0.87	0.83	0.84	0.79	0.81
C (s)	10.99	7.07	9.08	6.05	6.26
C^{-1} (s^{-1})	0.09	0.141	0.11	0.17	0.161
% Diff*	0.0	37.9	16.6	43.4	44.0
Correlation	0.9878	0.9893	0.9844	0.9902	0.9883
Variance	0.0028	0.0019	0.0035	0.0017	0.0019

* $\%\text{Diff} = \frac{\eta_{o,\text{Pure-HDPE}} - \eta_o}{\eta_{o,\text{Pure-HDPE}}}$

zero-shear and shear thinning viscosities of HDPE (Table II). The compatibilizer interaction with organoclay led to a 43.4% decrease in the zero-shear viscosity of HDPE. It should be noted that the compatibilizer alone caused a decrease of 37% in the zero shear viscosity of HDPE.

It is known that polymer extrusion involves a transient flow at high shear rates. So, a stress growth experiment was conducted to monitor the effect of organoclay on the normal stress differences of HDPE. Figure 8 showed that as the clay loading decreased from 0.1 to 0.05 wt %, the normal stress differences decreased. Hence, the lower the clay loading used in HDPE, the better the performance of the clay in the reduction of the normal force. Similar results as in the case of the steady shear rate tests were experienced when the compatibilizer was added during the growth test.

An abundance of experimental discussion was offered on shear rheology to arrive at a reasonable conclusion that organoclay had an effect on the linear and nonlinear shear rheology of HDPE. The results showed that the addition of organoclay reduced the linear viscoelastic behavior of HDPE especially after the crossover frequency. Also, the shear viscosity and normal stress difference of HDPE decreased when organoclay was added to it. The same trend was observed during stress growth test. However, no synergistic effect was noticed between the organoclay and PE-*g*-MA in the reduction of the shear behavior of HDPE.

Extensional rheology

The extensional effect of the organoclay and the compatibilizer on HDPE at 145°C and Hencky strain rate 10 s^{-1} was as shown in Figure 9. Strain hardening was observed in the plot of HDPE at this high Hencky strain rate. This is typical of linear polymer when subjected to high strain deformation near the polymer melt state. Both the organoclay and the compatibilizer reduced the extensional stress and strain within the polymer. For clay loading of 0.1 wt %, the maximum extensional stress developed in HDPE (at extensional strain of 4) decreased by

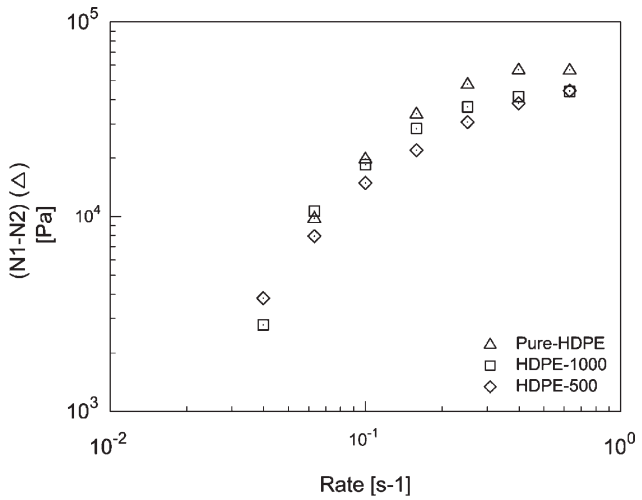

Figure 7 Effect of different clay loadings on the normal stress differences (N_1–N_2) of HDPE during steady shear rate sweep test in parallel plates.

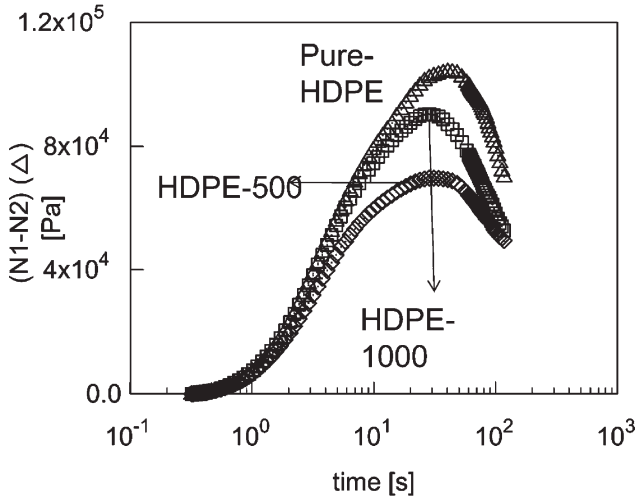

Figure 8 Effect of different clay loadings on the normal stress differences (N_1–N_2) of HDPE during stress growth test in parallel plates.

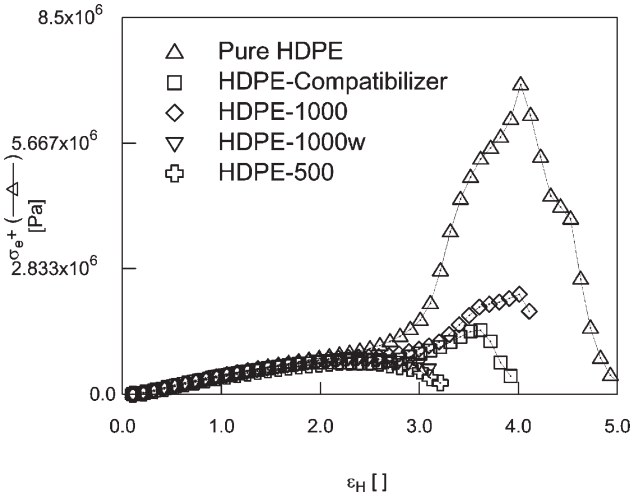

Figure 9 Effect of compatibilizer and different clay loadings on the extensional stress growth of HDPE.

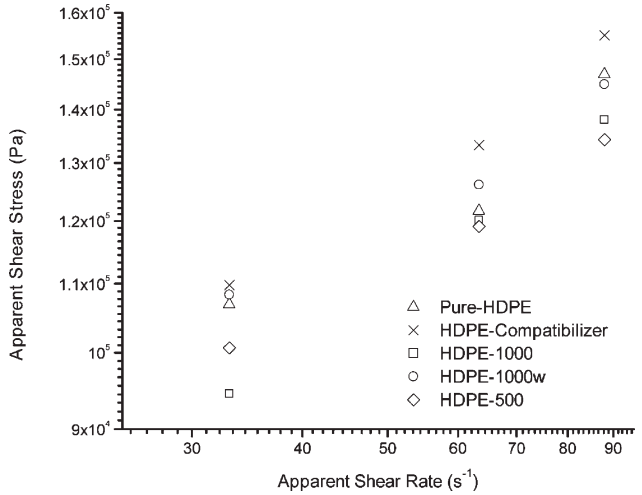

Figure 10 Flow curve for Pure-HDPE and different clay loadings' effects on HDPE during extrusion in the single screw extruder with slit die head.

68%. When the clay loading was further decreased to 0.05 wt %, a decrease of up to 89% was observed in the maximum extensional stress developed in HDPE. Such a decrease in extensional stress and strain indicated that organoclay was able to dissipate energy within the polymer as in the case of boron nitride.[39] It seemed the compatibilizer also assisted the organoclay to further decrease the maximum extensional stress in HDPE by 88%.

The results from the shear and extensional rheology indicated that both the organoclay and the compatibilizer had effects on the rheology of HDPE. However, their effects on extensional rheology were more than their impacts on shear rheology. It should be noted that the shear and extensional rheology were conducted at 200 and 145°C, respectively. This might be the reason for the larger reduction in extensional rheology as compared to shear rheology.

Since materials during continuous extrusion undergo shearing and elongation processes, the correlation between the rheology and extrusion should

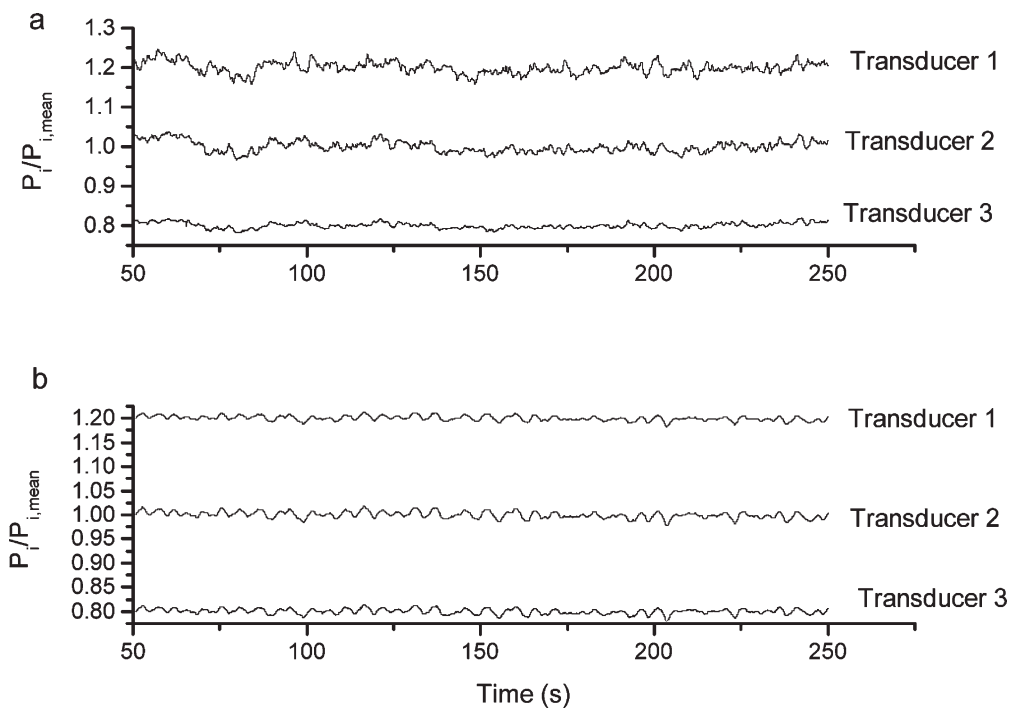

Figure 11 The associated normalized pressure fluctuations along the slit die at a shear rate of 63 s^{-1}. (a) For HDPE where gross melt fracture developed. (b) For HDPE-500 where 0.05 wt % addition of organoclay to HDPE eliminated the melt instability. Curves were shifted by ±0.2 in the vertical axes for better representation.

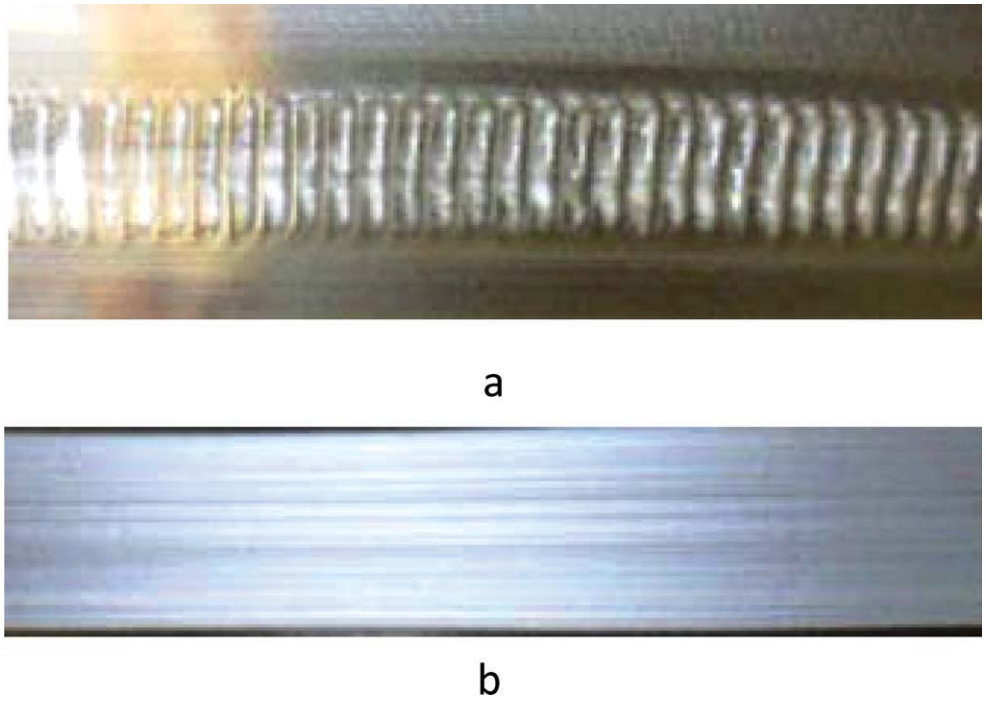

Figure 12 Visual Observation of (a) HDPE with gross melt fracture and (b) HDPE-500 without sharkskin at apparent shear rate of 63 s^{-1}. [Color figure can be viewed in the online issue, which is available at wileyonlinelibrary.com.]

be studied. Therefore, the next section will discuss how the compatibilizer and the organoclay affect instabilities in the extrusion of HDPE.

Extrusion processing

As earlier mentioned, the melt instability in HDPE during extrusion was studied in a single screw extruder with a slit die. At the processing temperature of 160°C, the extruded HDPE had gross melt fracture at all the attainable apparent shear rates. Figure 10 shows the flow curve for the HDPE and its organoclay nanocomposites. At the same apparent shear rate, the stress of HDPE became reduced in the presence of organoclay. This showed that organoclay as a processing aid in HDPE led to reduction in extrusion pressure. The intensity of the melt fracture in HDPE increased as the shear rate increased. The addition of organoclay (C15A) eliminated the melt fracture in HDPE. The elimination occurred at all the attainable shear rates in this experiment. High pressure fluctuation was an indication of gross melt fracture. For example, at a shear rate of 63 s^{-1}, typical recorded pressure fluctuations along the die with piezoelectric transducers were as shown in Figure 11. The corresponding visual observation of the extruded samples (Pure-HDPE and HDPE-500) was as presented in Figure 12. We observed that with the addition of organoclay, the pressure fluctuation along the die became reduced. Another striking point in Figure 11 was that these fluctuations occurred simultaneously. The in-phase between the pressure signals was confirmed with cross correlation analysis. The maximum in the cross correlation was at zero-time lag regardless of the

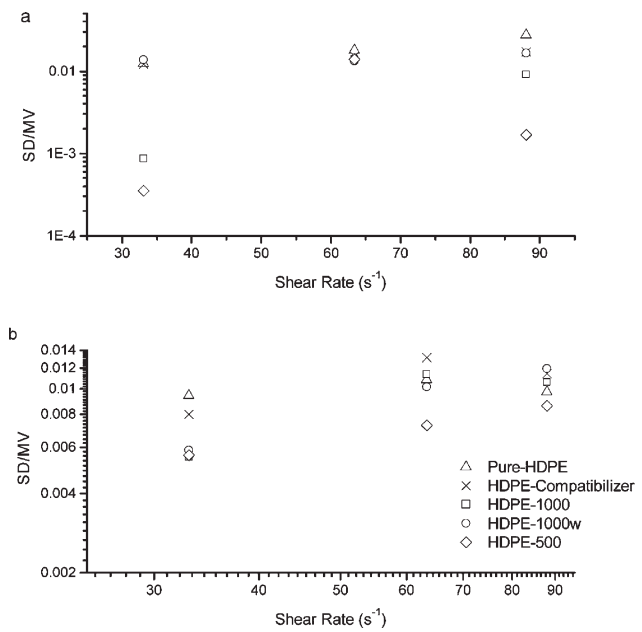

Figure 13 The effect of different clay loadings and compatibilizer on the pressure fluctuation measured as the ratio between the standard deviation of the pressure signal (SD) and its mean value (MV). (a) SD/MV versus shear rates at the entrance of the die. (b) SD/MV versus shear rates at the position P3 from the exit of the die.

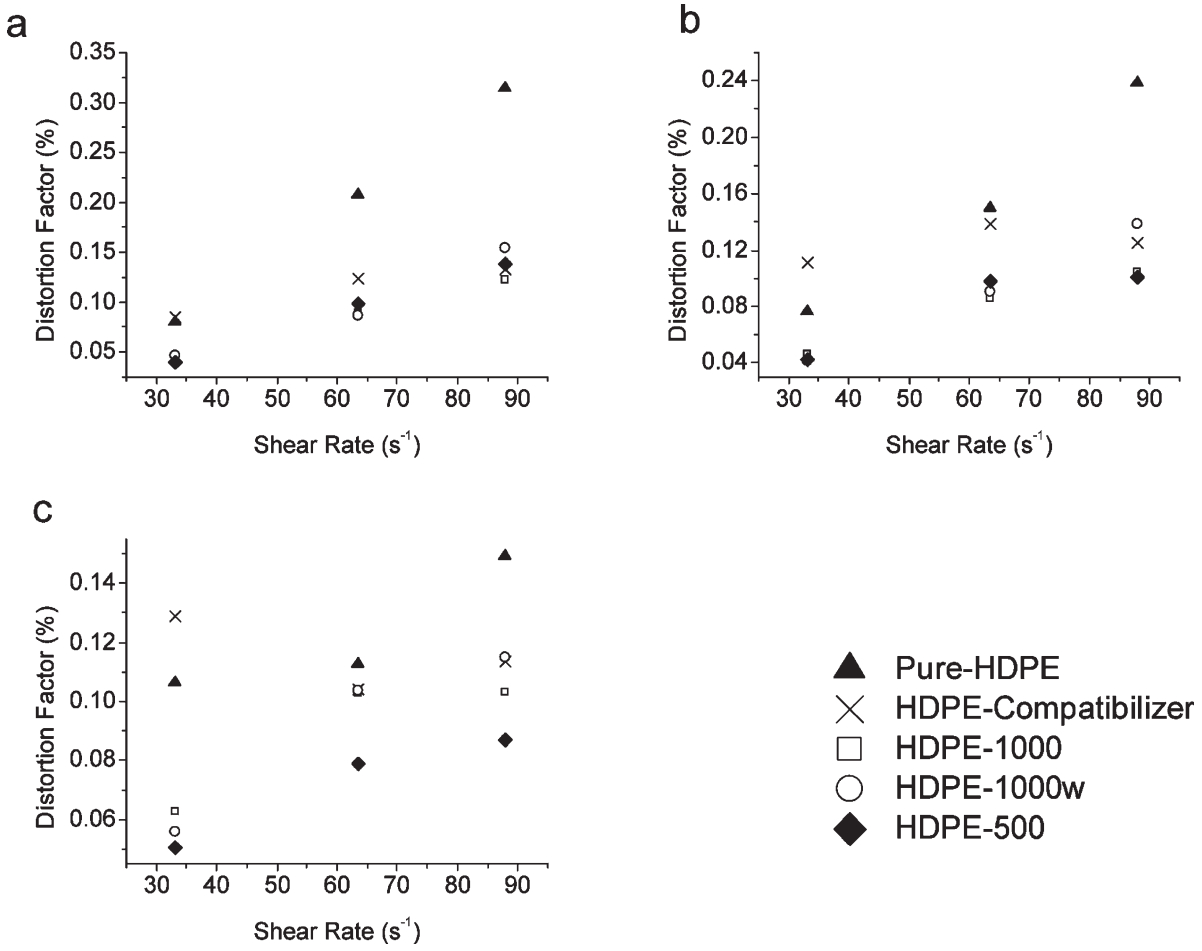

Figure 14 The effect of different clay loadings and compatibilizer on the pressure fluctuation measured with distortion factor (DF). (a) DF versus shear rate for transducer 1 at position P1. (b) DF versus shear rate for transducer 2 at position P2. (c) DF versus shear rate for transducer 3 at position P3.

pair of transducers analyzed. This implied that the gross melt fracture possibly originated from the entrance of the die producing a continuous fluctuating signal inside the die. To characterize the pressure fluctuations during the melt fracture and its attenuation, both moment analysis and distortion factor were used.

Figure 13 presented the effect of organoclay and the compatibilizer on the relative pressure fluctuations as measured by the ratio between standard deviation of the pressure signals and its mean value (SD/MV). It can be seen from the figure that an addition of 0.05 wt % organoclay to HDPE (HDPE-500) was most effective in reducing the intensity of the pressure fluctuations both at the entrance and exit of the die. The visual observation confirmed the trend showed in the figure. The addition of the compatibilizer alone did not help in the improvement of the extrusion of HDPE. As a result no reduction was seen in the SD/MV values of HDPE both at the entrance and exit of the die. Even though 0.1 wt % organoclay improved the glossiness of the HDPE extrudate, the addition of compatibilizer to it had no additional synergistic effect on the extrudate as confirmed in Figure 13. A distortion factor (DF) was used as defined in Eq. (6) to further quantify the generated pressure fluctuation. Generally, the DF decreased downwardly along the die as shown in Figure 14. The decrease indicated that HDPE became relaxed as it moved towards the die exit. This DF plot also confirmed that 0.05 wt % organoclay acted best in the attenuation of the pressure fluctuation. The reduction caused by 0.05 wt % organoclay was 2 decades less at low shear rate and a decade less at high shear rate (compare the DF values at shear rates 33 and 88/s, respectively). Both 0.1 wt % (HDPE-1000) and 0.05 wt % (HDPE-500) organoclay acted equally at the upstream of the die, hence similar DF values. However, at the die exit the DF of HDPE-500 was less than that of HDPE-1000. This difference might have contributed to the smoother surface of HDPE-500. This result could be expected because at the die exit there were other complicated phenomena such as a swelling phenomena and

normal forces which could contribute to melt instability. But with a reduction in the pressure fluctuation, such complications could possibly be reduced and hence eliminate or postpone gross melt fracture. Figure 14 also confirmed that the compatibilizer did not improve the action of organoclay—as a processing additive—in HDPE.

The observed improvement during the extrusion of HDPE was due to the effect of organoclay and not degradation due to processing. This was confirmed by conducting further dynamic frequency sweeps on the extrudates. The elastic and loss moduli of the samples before and after extrusion were found to be the same within the allowable error margins, which were less than 3%.

Relationship between rheology and processing of HDPE and its organoclay nanocomposites

The linear and nonlinear shear rheological studies showed that the elastic behavior of HDPE reduced with the addition of organoclay. This led to the decrease in nonlinear material properties like normal stress differences in steady shear and stress growth tests. Also, the extensional rheology showed that the extensional stress growth and strain in pure HDPE were reduced with the addition of organoclay and compatibilizer. All these rheological results showed why organoclay enhanced the HDPE processing during extrusion. The organoclay was able to streamline the polymer flow and hence its alignment in the flow direction. This alignment aided the elastic energy dissipation in HDPE. So, the addition of organoclay eliminated the gross melt fracture in the extruded HDPE and reduced the extrusion pressure. According to Larson[40] and Kissi et al.,[41] large normal stress differences are responsible for the solid-like fracture of molten polymers-gross melt fracture. Our work confirmed this proposition because the organoclay was able to reduce the normal stress differences and hence eliminated the gross melt fracture. This work confirmed the proven fact that an addition of organoclay leads to a reduction of extensional stress growth.[27] However, based on the new results of this study, it can be argued that the elimination or postponement of melt instabilities especially gross melt fracture was not only due to the decrease of extensional stress alone. The reduction of large normal stress differences due to preshearing of the samples at the upstream of the die entrance contributed to the elimination or postponement of the gross melt fracture as well. It is also possible that organoclay is playing the role of a plasticizer in HDPE.

Further dispersion of clay using a compatibilizer had no synergistic effect at low clay loading of 0.1 wt %. The observed reduction in the presence of compatibilizer was solely due to the dominant effect of PE-*g*-MA alone. Therefore, it can be concluded that master batching followed by the dilution of the organoclay in the HDPE caused the required amount of dispersion. Thus, it is enough to use the organoclay as a processing aid without a compatibilizer. This finding is of important industrial implications and can be implemented by adding small amounts of clay ($\sim$ 0.05 wt %) as an additive in the extrusion of polymer especially HDPE. The effectiveness of 0.05 wt % clay loading as compared to 0.1 wt % might be because of a difference in the size of the organoclay during its dispersion in HDPE. It is more likely that there was more agglomeration in HDPE-1000 when compared to HDPE-500.

CONCLUSION

The effect of organoclay on the rheology and extrusion of HDPE was studied. It was found that at clay loadings between 0.05 and 0.1 wt %, the shear and extensional rheology of HDPE were impacted. The elasticity of HDPE was reduced with the addition of organoclay as suggested by the data collected on the reduction of the normal stress differences of the polymer. Also, the organoclay was able to reduce the extensional stress growth and strain in HDPE. All these contributed to the ability of the organoclay to act as a good processing aid during HDPE extrusion. The gross melt fracture was eliminated with organoclay in a single-screw extruder. The intensity of the melt instabilities were characterized by both moment analysis and distortion factor. Both analyses showed that the organoclay reduced the intensity of pressure fluctuations along the die. Furthermore, this study showed that, at a low clay loading, the addition of a compatibilizer may not be necessary in the dispersion of organoclay when using a combination of master batching and dilution. Finally, this work concluded with the assertion that both shear and extensional rheology contributed to the melt instabilities observed in the extrusion of HDPE and such instabilities could be delayed by using small amounts of organoclay.

We thank Saudi Arabia Basic Industries (SABIC) for providing polymer samples for this work. We are also grateful to Dr. Anwar Ul-Hamid of the Research Institute at KFUPM for his tremendous assistance towards SEM testing.

References

1. Carreras, E. N.; Kissi, J.-M.; Piau, F. T.; Nigen, S. Rheol Acta 2006, 45, 209.
2. Evdokia, A.; Georgios, C. G.; Hatzikiriakos, S. G. Appl Rheol 2002, 12, 88.
3. Hatzikiriakos, S. G.; Migler, K. B. Polymer Processing Instabilities Control and Understanding; Marcel Dekker: New York, 2005.

4. Delgadillo-Velázquez, O.; Georgiou, G.; Sentmanat, M.; Hatzikiriakos, S. G. Polym Eng Sci 2008, 48, 405.
5. Mitsuyoshi, F.; Hitoshi, I. J Appl Polym Sci 2002, 84, 2111.
6. Mitsuyoshi, F.; Hitoshi, I. J Appl Polym Sci 2002, 84, 2120.
7. Palza, H.; Filipe, S.; Naue, I. F. C.; Wilhelm, M. Polymer 2010, 51, 522.
8. Anastasiadis, S. H.; Hatzikiriakos, S. G. J Rheology 1998, 42, 795.
9. Kolnaar, J. W. H.; Keller, A. J Non-Newtonian Fluid Mechanics 1997, 69, 71.
10. Pudjijanto, S.; Denn, M. M. J Rheology 1994, 38, 1735.
11. Perez-Gonzalez, J.; Denn, M. M. Ind Eng Chem Res 2001, 40, 4309.
12. Hatzikiriakos, S. G.; Peter, H.; Wally, H.; Charles, W. S. J Appl Polym Sci 1995, 55, 595.
13. Kazatchkov, I. B.; Hatzikiriakos, S. G.; Bohnet, N.; Goyal, S. K. Polym Eng Sci 1999, 39, 804.
14. Filipe, S.; Becker, A.; Barroso, C. V.; Wilhelm, M. Appl Rheol 2009, 19, 23345.
15. Hong, Y.; Cooper-White, J. J.; Mackay, M. E.; Hawker, C. J.; Malmstrom, E.; Rehnberg, N. J Rheol 1999, 43, 781.
16. Hong, Y.; Coombs, S. J.; Cooper-White, J. J.; Mackay, M. E.; Hawker, C. J.; Malmström, E.; Rehnberg, N. Polymer 2000, 41, 7705.
17. Hatzikiriakos, S. G.; Kazatchkov, I. B.; Vlassopoulos, D. J Rheol 1997, 41, 1299.
18. Xing, K. C.; Schreiber, H. P. Polym Eng Sci 1996, 36, 387.
19. Migler, K. B.; Lavallee, C.; Dillon, M. P.; Woods, S. S.; Gettinger, C. L. J Rheol 2001, 45, 565.
20. Kharchenko, S. B.; McGuiggan, P. M.; Migler, K. B. J Rheol 2003, 47, 1523.
21. Franky, Y.; Hatzikiriakos, S. G.; Thomas, M. C. J Vinyl Additive Technol 2000, 6, 113.
22. Eugene, E. R.; Stuart, K. R.; Hatzikiriakos, S. G.; Charles, W. S.; Donald, L. H.; Marlin, B. Polym Eng Sci 2000, 40, 179.
23. Manish, S.; Hatzikiriakos, S. G.; Thomas, M. C. Polym Eng Sci 2002, 42, 743.
24. Kazatchkov, I. B.; Yip, F.; Hatzikiriakos, S. G. Rheol Acta 2000, 39, 583.
25. Palza, H.; Reznik, B.; Kappes, M.; Hennrich, F.; Naue, I. F. C.; Wilhelm, M. Polymer 2010, 51, 3753.
26. Kharchenko, S. B.; Douglas, J. F.; Obrzut, J.; Grulke, E. A.; Migler, K. B. Nat Mater 2004, 3, 564.
27. Hatzikiriakos, S. G.; Nimish, R.; Edward, B. M. Polym Eng Sci 2005, 45, 1098.
28. Manish, S.; Hatzikiriakos, S. G. J Vinyl Additive Technol 2001, 7, 90.
29. Kim, Y. C.; Yang, K. S. Polym J 1999, 31, 579.
30. Muliawan, E. B.; Rathod, N.; Hatzikiriakos, S. G.; Sentmanat, M. Polym Eng Sci 2005, 45, 669.
31. Lee, S. M.; Lee, J. W. In Proceeding ANTEC, Technical Paper; New York, USA, 2001.
32. Seth, M.; Yip, F.; Hatzikiriakos, S. G. In Proceeding ANTEC, Technical Paper; Dallas, TX, 2000, p 2649.
33. Yip, F.; Diraddo, R.; Hatzikiriakos, S. G. J Vinyl Additive Technol 2000, 6, 196.
34. Kim, Y. C.; Lee, S. J.; Kim, J. C.; Cho, H. Polym J 2005, 37, 206.
35. Hotta, S.; Paul, D. R. Polymer 2004, 45, 7639.
36. Százdi, L.; Ábrányi, Á.; Pukánszky, B.; Vancso, J. G. Macromol Mater Eng 2006, 291, 858.
37. Macosko, C. W. Rheology Principles, Measurements, and Applications; Wiley-VCH: New York, 1994.
38. Filipe, S.; Vittorias, I.; Wilhelm, M. Macromol Mater Eng 2008, 293, 57.
39. Sentmanat, M.; Hatzikiriakos, S. G. Rheol Acta 2004, 43, 624.
40. Larson, R. G. Rheol Acta 1992, 31, 213.
41. Kissi, N. E.; Léger, L.; Piau, J. M.; Mezghani, A. J Non-Newtonian Fluid Mechanics 1994, 52, 249.